Sivakumar, V. *et al.* (2010). *Géotechnique* **60**, No. 8, 581–594 [**doi:** 10.1680/geot.8.P.007]

Mechanical behaviour of unsaturated kaolin (with isotropic and anisotropic stress history). Part 1: wetting and compression behaviour

V. SIVAKUMAR*, R. SIVAKUMAR†, E. J. MURRAY‡, P. MACKINNON* and J. BOYD§

Over the last 40 years considerable progress has been made in understanding the complex behaviour of unsaturated soils. Research using constitutive modelling has extended the critical state framework and the concept of yielding in saturated soils to encompass unsaturated soils experiencing suction. However, validation testing of the framework for unsaturated soils has shown disagreement with the basic propositions. The main reason for this disparity is the anisotropic properties of the soil specimens tested as a result of preparation using one-dimensional compaction. The paper describes the detailed testing carried out to justify this statement. As part of the work presented, samples of unsaturated kaolin were prepared using isotropic compression. The suctions in these samples were reduced to predefined values by wetting under low isotropic loading. The pore size distributions, the pressure–volume relationships and yielding under subsequent isotropic loading are compared with tests on samples prepared by statically compressing kaolin into a one-dimensional compaction mould. The anisotropically compressed samples had initial water contents and specific volumes similar to those of the isotropically prepared samples and were also tested under reducing suctions; they exhibited distinctly different behaviour when tested under similar conditions. The results obtained from the isotropically prepared and tested samples have shown, probably for the first time, the existence of a unique normal compression surface that is not dependent on the initial conditions of the samples. The shape of the loading–collapse (LC) yield locus is shown to be different from the generally accepted form.

KEYWORDS: anisotropy; clays; compaction; earth fill; laboratory tests; stress path

Au cours des 40 dernières années, on a réalisé des progrès considérables dans la compréhension du comportement complexe des « sols non saturés ». Des travaux de recherche faisant usage d'une modélisation constitutive ont déterminé l'expansion du cadre de l'état critique ainsi que le concept de l'affaissement dans les sols saturés, en incorporant les sols non saturés soumis à une aspiration. Toutefois les essais de validation du cadre relatif aux sols non saturés présentent des divergences avec les thèses de base. La principale raison de cette disparité tient aux propriétés anisotropes des spécimens de sol testés en conséquence de la préparation faisant usage d'un compactage unidimensionnel. La présente communication décrit les essais détaillés qui ont été effectués à l'appui de cette thèse. Dans le cadre des travaux présentés, on prépare des échantillons de kaolin non saturé par compression isotrope. On compare ensuite la distribution des diamètres de pores, les rapports pression /volume et le fléchissement sous l'effet des charges isotropes ultérieures avec des tests effectués sur des échantillons préparés par la compression statique de kaolin dans un moule de compactage unidimensionnel. Initialement, la teneur en eau et le volume massique des échantillons à compression anisotrope sont similaires à ceux des échantillons ayant fait l'objet d'une préparation isotrope, et ces échantillons sont soumis à des tests avec réduction de l'aspiration, et présentent un comportement nettement différent lorsqu'ils sont soumis à des tests dans des conditions similaires. Les résultats obtenus sur des échantillons à préparation isotrope et soumis à des tests présentent, probablement pour la première fois, l'existence d'une surface de compression normale unique, qui n'est pas tributaire de l'état initial des échantillons. On démontre que la forme du locus de fluage de la charge d'affaissement LC se distingue de la forme traditionnellement reconnue.

INTRODUCTION

The development of a critical state framework for saturated soils provides a powerful conceptual model based on the generalised principles of the elastoplastic behaviour of frictional materials (Schofield & Wroth, 1968). The model has been modified with time to meet the requirements of more complex applications (Muir Wood, 1990; Wheeler, 1997). Alonso *et al.* (1987) were among the first researchers to propose an elasto-plastic model for unsaturated soils which was subsequently fully developed by Alonso *et al.* (1990). The model was later evaluated by Wheeler & Sivakumar (1995). The model uses the five state variables listed below and incorporates the concept of the two stress state variables (Matayas & Rahadakishna, 1968)

$$\overline{p} = \frac{\sigma_1 + 2\sigma_3}{3} - u_a \tag{1}$$

$$q = \sigma_1 - \sigma_3 \tag{2}$$

$$s = u_a - u_w \tag{3}$$

$$v = 1 + e \tag{4}$$

$$v_w = 1 + wG_s \tag{5}$$

where $\overline{p}$ q, s, v and v_w are the mean net stress, deviator stress, suction, specific volume and specific water volume respectively, and u_a, u_w, σ_1, σ_3, e, w and G_s are pore air pressure, pore water pressure, major principal stress, minor principal stress, void ratio, water content and specific gravity respectively.

The model proposed by Alonso *et al.* (1990) and enhanced by Wheeler & Sivakumar (1995) suggested the existence of an isotropic normal compression surface in $\overline{p}$, s, v space, critical state surface in $\overline{p}$, q, s and $\overline{p}$ s, v spaces

Manuscript received 21 January 2008; revised 15 June 2009. Published online ahead of print 12 March 2010.
Discussion on this paper closes on 1 January 2011, for further details see p. ii.
* School of Planning, Architecture and Civil Engineering, Queen's University Belfast, Belfast, UK.
† Atkins, Epsom, UK
‡ Murray Rix Geotechnical, Warwickshire, UK.
§ University of Ulster, UK.

and a state boundary hyper-surface in $\overline{p}$, *q, s,* v hyper-space. Similar surfaces and hyper-surfaces have also been proposed in relation to specific water volume v_w (Wheeler & Sivakumar, 1995). The soil behaviour is assumed to be elastic if the state of the soil lies inside the state boundary hyper-surface. On the surface both elastic and plastic deformations occur.

Thermo-dynamic principles and the Cam-Clay model of Schofield & Wroth (1968) are generally used to explain the concepts of the elastic domain and yielding in saturated soils. The extension of the concepts to unsaturated soils, taking account of suction effects, produces a yield surface in $\overline{p}$, *q, s* space as shown in Fig. l(a). The intersection of this surface on the $q = 0$ plane produces the loading–collapse (LC) yield locus on the $\overline{p}$:*s* plane as illustrated in Fig. 1(b). Any change in either of the two stress state variables within the LC yield locus (path ABC or PBQ) produces elastic volume change; and when the stress state exceeds the LC yield locus, plastic hardening occurs. The pressure–volume relationship ($\overline{p}$ expressed on logarithmic scale) of a path ABCD where the suction is held constant is presented in Fig. 1(c). Along the path ABC the soil is assumed to behave elastically and along the path CD is assumed to behave in an elasto-plastic manner. According to the principles of the Cam-Clay model, the state of the soil when undergoing yielding is unique and unaffected by the initial condition of the soil, assuming that the effects of cementation and bonding are neglected. The existence of a unique state for an unsaturated soil when yielding does not appear to have been contested.

Sivakumar & Wheeler (2000) reported results obtained from samples of kaolin statically compressed into a one-dimensional mould to two different initial densities. The work showed that the state of the unsaturated soils when undergoing isotropic hardening was influenced by the initial condition of the samples. Tests on samples compacted or compressed one-dimensionally into a mould generally formed the basis of past research (Sivakumar, 1993; Cui & Delage, 1996; Sharma, 1998; Sivakumar & Wheeler, 2000; Wheeler & Sivakumar, 2000; Wang *et al.*, 2002; Tan, 2004). This process inevitably introduces a degree of stress-induced anisotropy in the samples, and a complex soil fabric. In saturated soils the stress-induced anisotropy results in the yield locus in the q:p' plane (where p' is mean effective stress) no longer being centred about the p' axis but approximately aligned to the K_0 axis, where K_0 is the coefficient of earth pressure at rest (Graham & Houlsby, 1983; Leroueil & Vaughan, 1990; Sivakumar *et al.*, 2002). There is evidence to suggest that the yield locus in the q: $\overline{p}$ plane for unsaturated soils may also no longer be aligned around the $\overline{p}$ axis (Delage & Graham, 1995). In this case, plastic strains are often generated by both rotational hardening (Wheeler, 1997) and volumetric hardening (Schofield & Wroth, 1968). The magnitude of the rotational hardening is influenced by the initial anisotropy in the soil. Therefore validation of the constitutive model for unsaturated soils requires, as a first step, the analysis of data from tests on soils with isotropic stress–strain properties. The model requires that for such soils the yield locus in the q: $\overline{p}$ plane should be symmetrical around the $\overline{p}$ axis if the rationale behind constitutive modelling of unsaturated soils is to be verified. However, it should be acknowledged that tests on initially isotropic samples do not guarantee the above requirements. For example, an initially isotropic sample that has undergone shear loading (not necessarily to failure) may develop anisotropic stress–strain properties and consequently the yield locus may not be symmetrical about the $\overline{p}$ axis. Any subsequent isotropic loading on the sample may exhibit anisotropic behaviour.

EXPERIMENTAL WORK

Sample preparation plays an important role in the modelling of unsaturated soils (Gens & Alonso, 1992; Maãtouk *et al.*, 1995; Sivakumar & Wheeler, 2000). In order to isolate the influence of stress-induced anisotropy on the behaviour of unsaturated soils, samples have been prepared with isotropic stress history. The following describes the methodology adopted in preparing isotropically and one-dimensionally prepared samples.

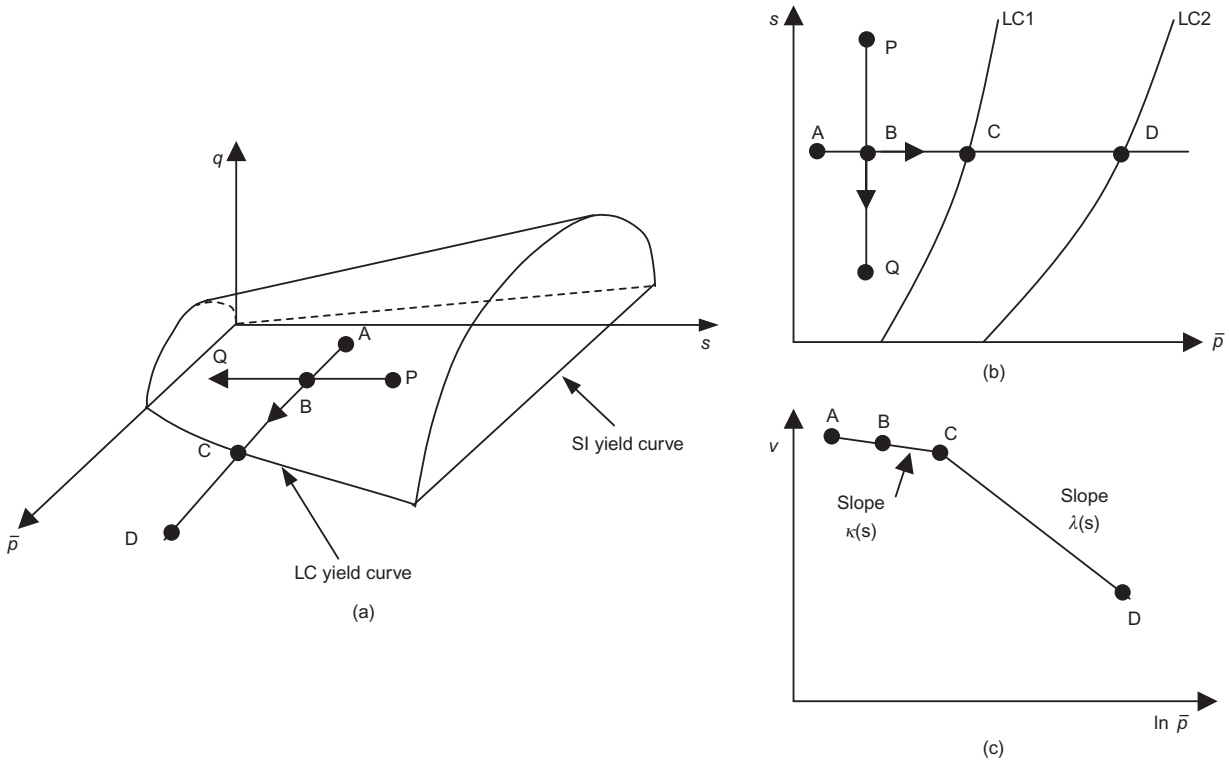

Fig. 1. Yielding of unsaturated soils

Sample preparation

Isotropically prepared samples: Wet kaolin at a targeted water content of 25% was prepared using the procedure described by Sivakumar (1993). The material was then passed through a sieve with an aperture size of 1·18 mm and sealed in a plastic bag for 48 h prior to sample preparation. A 100 mm diameter rubber membrane was placed around the pedestal of a standard triaxial cell and sealed to the base using two O-rings. A membrane stretcher was placed around the membrane and the top of the membrane was folded at the top of the stretcher. A 100 mm diameter dry porous disc was placed on the pedestal and the sieved material was filled slowly into the membrane. With the membrane full, a top cap with a dry porous stone was placed on the kaolin, the membrane stretcher was removed and the top cap was sealed with two O-rings. The cell was assembled and pressurised to the required value. Any excess air pressure, developed as a result of the application of the external pressure, was allowed to dissipate from the top and bottom of the sample. There was no evidence of water drainage during this process. Although consolidation usually took place quickly, the sample was left in the compression system for three days as a standard procedure. At the end of this time the confining pressure was reduced to zero and a thin wall sample tube was used to extract a sub-sample of 50 mm diameter and 100 mm height.

Figure 2 shows the compression pressure–specific volume relationship of the unsaturated soil samples prepared at a water content of 25%. Note that no attempt was made to measure suction during the compression of the wet kaolin in the chamber and therefore the pressure–volume relationship shown in Fig. 2 does not represent constant suction conditions. The research was primarily aimed at assessing the influence of stress-induced anisotropy on the performance of unsaturated soils and to allow comparison with published data. Samples were prepared at targeted initial specific volumes of 2·19 and 1·99, which are the initial conditions of the samples prepared by Wheeler & Sivakumar (1995) and Sivakumar & Wheeler (2000) using one-dimensional compression at a water content of 25%.

One-dimensionally compressed samples

Sivakumar & Wheeler (2000) and Wheeler & Sivakumar (1995) reported test data generated on samples that were prepared using one-dimensional compression. These tests were performed under controlled suction, and no attempt was made to perform tests under constant water mass conditions, where no drainage of water was allowed. Therefore, to supplement the published results, further tests were performed with the samples prepared by one-dimensional compression in nine layers with each layer compressed to give a specific volume of 2·19 and these samples were tested under constant water mass conditions.

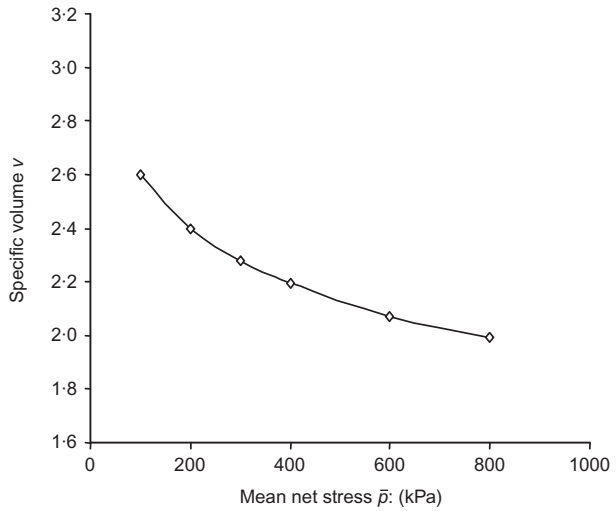

Fig. 2. Pressure–volume relationship under constant water mass loading

Test procedures

The following describes the two basic test procedures employed and referred to in the subsequent text.

Controlled suction tests. Tests were performed in a twin-cell stress path apparatus. A detailed description of this apparatus is reported in Sivakumar *et al.* (2006). Suction was controlled using the axis translation technique originating from Hilf (1956). The samples were initially wetted to pre-selected values of suction and subsequently isotropically compressed under constant suction.

Constant water mass tests. In the constant water mass tests, a thermocouple psychrometer was used to measure changes in the soil suction. The psychrometer tip was attached to the top loading cap and a small hole was drilled in the top of the sample to allow the tip to be seated properly when the cell was assembled. Other than the psychrometer, all the instrumentation readings were monitored using Lap-PC software. The psychrometer readings were calibrated using sodium chloride (NaCl) solutions prepared at different concentrations (Comstock, 2000) with correction for temperature effects. Further details on this can be found in Thom *et al.* (2008). The samples were initially isotropically compressed to pre-selected values of $\overline{p}$ and then sheared under constant water mass conditions.

Mercury intrusion porosimetry. As part of the study, the pore size distributions of both isotropically and one-dimensionally prepared samples before and after wetting to full saturation were determined using mercury intrusion porosimetry (MIP). Small cubic specimens of approximately 10 mm side were carefully cut from the samples that were prepared using the various procedures described above. The prepared specimens were freeze-dried using the method described by Ahmed *et al.* (1974), which involved quick freezing of the soil specimen to cryogenic temperatures of below −130°C, to avoid formation of crystalline ice, by direct immersion in liquid nitrogen. Following freezing, the water in the specimens was removed by sublimation using a true vacuum at a temperature between −60°C and −80°C. This process of dehydration prevents air–water menisci from forming as the water is removed. The freeze-dried specimens were wrapped in cling film and kept in air-tight plastic bags prior to carrying out the MIP tests (D 4404-84, ASTM, 2004), which were performed in the Geotechnical Laboratory of Durham University. The mercury chamber was initially calibrated for apparent volume change in which the pressure of the mercury was increased in steps up to 6120 kPa (steps of 68 kPa up to 680 kPa and then steps of 680 kPa up to 6120 kPa). A similar procedure was repeated when the sample was in the mercury chamber and each pressure increment was maintained constant until no significant volume of mercury entered into the chamber. The difference between the two volume change measurements is assumed to be the volume of mercury intruded into the pores of the dry kaolin sample at the specified pressure. The pore diameters were calculated using the method proposed by Washburn (1921).

RESULTS AND DISCUSSION

All the test data reported are for samples prepared at a water content of 25%, which is approximately 4% drier than the optimum water content measured using standard Proctor compaction. The samples prepared using isotropic compression to average initial specific volumes of 2·19 (lightly compressed) and 1·99 (heavily compressed) are identified as IS(A) and IS(B) respectively. The initial condition of each sample is listed in Table 1. The data obtained from one-dimensionally compressed samples (Wheeler & Sivakumar, 1995; Sivakumar & Wheeler, 2000) are represented by ID(A) and ID(B). In these two cases, ID(A) and ID(B), the initial specific volumes were the same as those of samples prepared using isotropic compression IS(A) and IS(B) respectively. The initial conditions of these samples are listed in Table 2. The following aspects of the test results are discussed in detail

(*a*) wetting-induced volume change of isotropically prepared samples under low isotropic stress conditions
(*b*) pore-size distribution of isotropically prepared samples following wetting
(*c*) effects of stress-induced anisotropy on the volume change of samples during wetting
(*d*) effects of stress-induced anisotropy on the pore-size distribution of samples following wetting
(*e*) pressure–volume relationships during isotropic compression under controlled and variable suctions of samples prepared isotropically
(*f*) effects of stress-induced anisotropy on the pressure–volume relationship and yielding.

Wetting-induced volume change of isotropically prepared samples under low isotropic stress conditions

The controlled suction tests performed on samples IS(A) and IS(B) are discussed. The initial suctions in the samples were 970 kPa and 850 kPa for IS(A) and IS(B) respectively. As part of the study, the suctions in the samples were reduced to pre-selected values of 300 kPa, 200 kPa and 100 kPa under an isotropic net stress of 50 kPa and in the case of zero suction under an isotropic net stress during wetting of 40 kPa. The reduction of the suction in the samples from the initial values resulted in an increase of the water content. Fig. 3 shows the changes in specific volume and specific water volume against the square root of time during the equalisation stage for a suction of 200 kPa for sample IS(A). The variations in v and v_w at the end of the wetting processes were approximately $\pm$ 0·007.

Figure 4 shows the specific water volume and specific volume of the samples of both series of tests at the end of the equalisation process plotted against the natural logarithm of $(s + p_{-atm})/p_{-atm}$· p_{-atm} (atmospheric pressure) is included to avoid the natural logarithm of suction becoming indeterminate when the suction falls to zero. The samples of both series had the same initial specific water volumes (represented by open data points for A and B), as they were prepared at the same target water content of 25%. The specific water volume plots for the two series of tests are similar until the suction drops below 100 kPa. However, there is a significant difference in the specific water volumes when the suction drops from 100 kPa to zero. At the higher values of suction the water that enters the samples predominantly occupies the micro voids within the aggregates where it is drawn by the effect of suction and only when the suction drops to low values are the macro voids filled. This behaviour is also evident in the soil water characteristic curves (WRC) of fine-grained soils which exhibit a bimodal pore size distribution. The pore sizes of aggregates are small and in the tests on kaolin were generally saturated within the suction range considered (more details on this aspect will be given later). However, the inter-aggregate voids are much larger and only flood with water at relatively low suctions.

Table 1. State parameters after sample preparation and normally consolidated state (isotropically prepared samples)

Test No.	After sample preparation		After equalisation				After isotropic compression			
	v	v_w	$\overline{p}$: kPa	s: kPa	v	v_w	s: kPa	$\overline{p}$: kPa	v	v_w
Samples of IS(A)										
1A	2·197	1·670	40	0	2·287	2·287	0	50	2·268	2·268
1B	2·194	1·669	40	0	2·288	2·299	0	100	2·146	2·146
1C	2·192	1·667	40	0	2·282	2·295	0	150	2·073	2·073
1D	2·193	1·662	40	0	2·278	2·274	0	307	2·018	2·018
2A	2·200	1·663	50	100	2·233	1·922	100	100	2·196	1·917
2B	2·186	1·652	50	100	2·242	1·921	100	150	2·161	1·927
2C	2·190	1·657	50	100	2·239	1·920	100	200	2·104	1·906
2D	2·194	1·662	50	100	2·247	1·934	100	310	2·047	1·884
3A	2·196	1·660	50	200	2·246	1·839	200	200	2·171	1·832
3B	2·195	1·652	50	200	2·249	1·842	200	150	2·216	1·842
3C	2·196	1·656	50	200	2·241	1·848	200	150	2·180	1·843
3D	2·202	1·656	50	200	2·246	1·846	200	350	2·044	1·832
4A	2·193	1·664	50	300	2·238	1·759	300	100	2·230	1·759
4B	2·197	1·667	50	300	2·239	1·766	300	100	2·233	1·761
4C	2·197	1·663	50	300	2·235	1·767	300	150	2·211	1·764
4D	2·202	1·656	50	300	2·231	1·759	300	350	2·107	1·750
Samples of IS(B)										
1	1·996	1·662	40	0	2·167	2·167	0	431	1·941	1·990
2	1·990	1·660	50	100	2·083	1·936	100	830	1·847	1·834
3	1·997	1·652	50	200	2·075	1·860	200	620	1·932	1·823
4	1·987	1·649	50	300	2·055	1·772	300	900	1·884	1·739

Table 2. State parameters after sample preparation and normally consolidated state (one-dimensionally prepared samples)

Test No.	After sample preparation		After equalisation				After isotropic compression			
	v	v_w	$\overline{p}$: kPa	s: kPa	v	v_w	s: kPa	$\overline{p}$: kPa	v	v_w
Samples of ID(A)										
1A	2·204	1·646	40	0	2·150	2·150	0	175	1·987	1·987
1B	2·197	1·650	40	0	2·160	2·160	0	200	1·975	1·975
1C	2·209	1·651	40	0	2·156	2·156	0	55	2·115	2·115
1D	2·208	1·652	40	0	2·136	2·136	0	100	2·038	2·038
1E	2·207	1·643	40	0	2·133	2·133	0	200	1·954	1·954
1F	2·000	1·650	40	0	2·115	2·115	0	150	2·008	2·008
1G	2·000	1·652	40	0	2·151	2·151	0	150	2·005	2·005
1H	2·191	1·649	40	0	2·149	2·149	0	75	2·079	2·079
2A	2·199	1·644	50	100	2·200	1·852	100	150	2·042	1·840
2B	2·213	1·644	50	100	2·214	1·852	100	100	2·133	1·852
2C	2·203	1·651	50	100	2·204	1·855	100	200	1·998	1·845
2D	2·207	1·640	50	100	2·198	1·850	100	150	2·038	1·849
2E	2·195	1·659	50	100	2·205	1·846	100	100	2·129	1·847
2F	2·209	1·638	50	100	2·205	1·842	100	150	2·046	1·841
3A	2·213	1·648	50	200	2·211	1·767	200	150	2·105	1·765
3B	2·195	1·649	50	200	2·213	1·770	200	100	2·162	1·781
3C	2·208	1·654	50	200	2·198	1·779	200	200	2·067	1·783
3D	2·209	1·647	50	200	2·220	1·788	200	150	2·127	1·784
3E	2·217	1·644	50	200	2·225	1·778	200	300	1·990	1·776
3F	2·209	1·643	50	200	2·216	1·770	200	100	2·172	1·771
3G	2·215	1·637	50	200	2·228	1·781	200	200	2·065	1·772
3H	2·207	1·645	50	200	2·202	1·769	200	150	2·099	1·779
4A	2·205	1·658	50	300	2·218	1·713	300	250	2·053	1·725
4B	2·202	1·654	50	300	2·209	1·727	300	100	2·195	1·712
4C	2·000	1·648	50	300	2·205	1·726	300	100	2·188	1·726
4D	2·201	1·652	50	300	2·208	1·726	300	150	2·140	1·729
Samples of ID(B)										
1A	1·976	1·667	40	0	2·078	2·078	0	150	1·969	1·969
1B	1·972	1·666	40	0	2·068	2·068	0	100	2·023	2·023
2A	1·983	1·660	75	100	2·023	1·827	100	200	1·958	1·819
2B	1·985	1·668	50	100	2·030	1·839	100	150	1·982	1·834
2C	1·983	1·668	50	100	2·040	1·838	100	125	2·008	1·832
3A	1·977	1·668	50	300	1·994	1·725	300	150	1·978	1·722
3B	1·977	1·666	50	300	2·002	1·725	300	175	1·979	1·719
3C	1·978	1·664	50	300	2·003	1·727	300	175	1·983	1·719

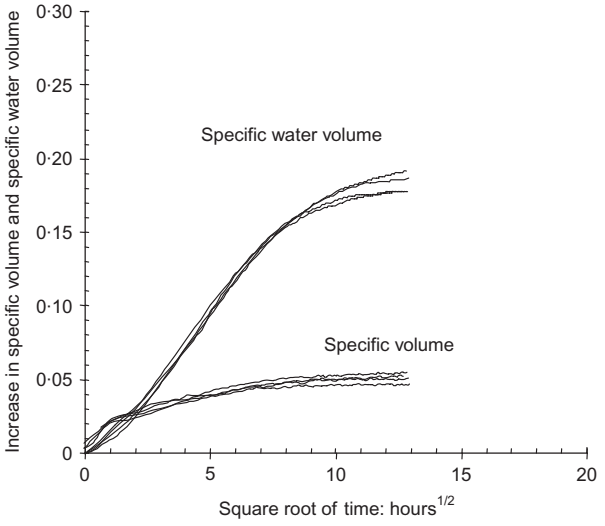

Fig. 3. Specific volume and specific water volume change during equalization $s = 200$ kPa for IS(A)

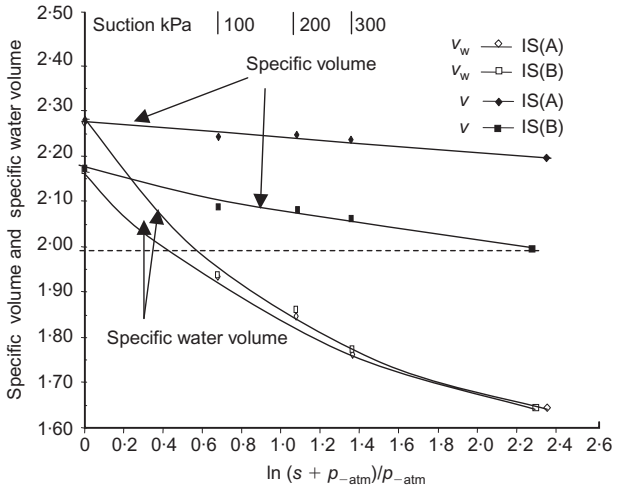

Fig. 4. Suction-volume and suction-water volume relationship

The pore size distribution of unsaturated soils is generally bimodal comprising: a microstructure associated with the distribution of relatively small intra-aggregate void spaces within the particle aggregations; and a macrostructure associated with larger inter-aggregate void spaces between the aggregates (Ahmed *et al.*, 1974; Alonso *et al.*, 1995; Wan *et al.*, 1995; Delage *et al.*, 1996). Fig. 5 shows the initial pore size distributions for IS(A) and IS(B). The pore size that separates the inter-aggregate voids and intra-aggregate voids is about 2 μm which is the average particle size of kaolinite. Since the samples were prepared to the same initial specific water volume, it is not surprising that the initial intra-aggregate voids (< 2 μm) for samples IS(A) and IS(B) are roughly similar. However, there is a marked difference between the macro-void spaces for IS(A) and IS(B). IS(A) was less compact, with a greater specific volume and suction. Essentially, greater compression for IS(B) resulted in the closure of the macro inter-aggregate void spaces.

The suctions in the samples of IS(A) and IS(B) reduced as the samples imbibed water and the equalisation processes progressed. This resulted in overall volume change of the soil. The specific volume responses of the soil samples are shown by the closed data points in Fig. 4. According to Alonso *et al.* (1995) and Sivakumar *et al.* (2006), there are three mechanisms involved in the volume change characteristics of unsaturated soils

(*a*) swelling of individual aggregates owing to water uptake
(*b*) aggregate slippage at the inter-aggregate contacts owing to lack of strength to support the externally applied load, leading to collapse compression
(*c*) distortion of aggregates into the inter-aggregate pore spaces.

The relative influence of these controlling factors determines the overall response of the unsaturated clay during wetting. None of the samples exhibited wetting-induced collapse compression, and the rate of swelling increased slightly with decreasing suction. The amounts of swelling in terms of changes in specific volume from the initial conditions are approximately 0·089, 0·048, 0·049 and 0·038 for IS(A) and 0·179, 0·093, 0·078 and 0·068 for IS(B) at zero, 100 kPa, 200 kPa and 300 kPa of suction respectively. The conditions of the sample after equalisation are listed in Table 1. Samples of both IS(A) and IS(B) exhibited a significant amount of swelling during the wetting process. While the reason for wetting-induced swelling can be explained by the fact that the wetting paths of both IS(A) and IS(B) were inside the LC yield locus, it is important to recognise that IS(B) swelled twice as much as IS(A). The same material (kaolin) was used in preparing samples IS(A) and IS(B) and both were prepared at an identical water content; the only preparation difference was the initial compression which will have resulted in differences in fabric structure. The observed differences in the swelling characteristics conflict with the proposal that the elastic volume change during wetting is given by equation (6), where κ_s, the swelling gradient with respect to suction, is generally assumed constant for monotonic wetting for a given material

$$\delta v = \kappa_s \frac{\delta s}{s + s_{ref}} \tag{6}$$

where s_{ref} is a reference suction. In the present study the wetting path under mean net stress of 50 kPa remained inside the yield locus indicated by 'no collapse' settlement in both IS(A) and IS(B). These samples were initially compressed to 400 kPa and 800 kPa respectively. The suction value at the sampling stage was in the order of 900 kPa. However the volume change (swelling) during the wetting of IS(B) was much higher than IS(A) implying that κ_s is not constant. The reason for the difference in κ_s can be explained using the results from MIP tests, which are discussed in the following section.

Pore-size distribution of isotropically prepared samples following wetting

Figures 6(a) and 6(b) show the pore size distributions of samples IS(A) and IS(B) which were allowed to saturate by reducing the suction to zero. Also included in the figures are

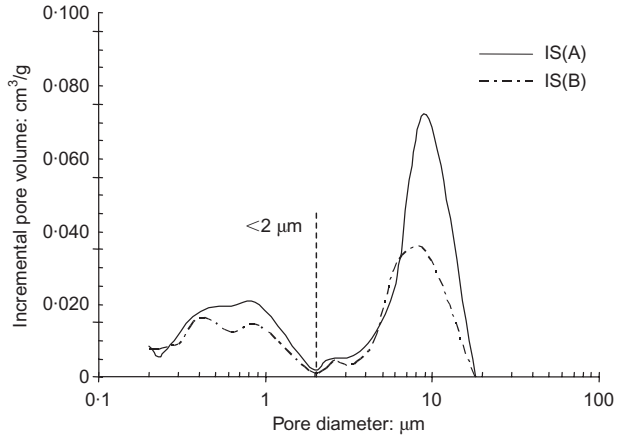

Fig. 5. Pore size distribution of unsaturated soils

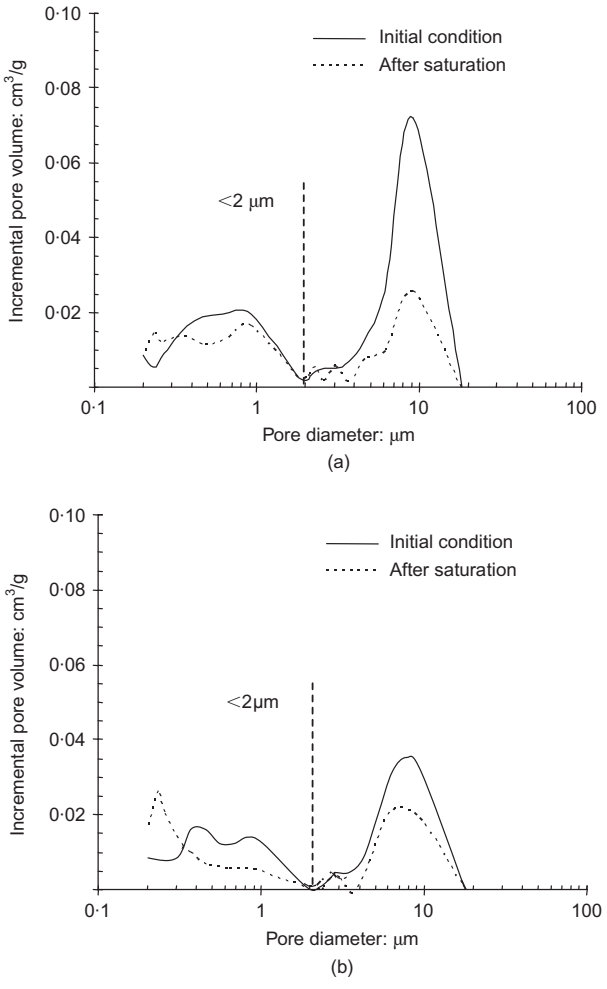

Fig. 6. Pore size distributions of (a) lightly compressed sample IS(A) and (b) heavily compressed sample IS(B)

the original pore size distributions of samples prior to being taken through the wetting process. In the case of the initially lightly compressed specimen IS(A), the maximum incremental pore volume of approximately 0·075 cm^3/g at pore size of 10 μm, which represents the inter-aggregate void spaces, reduced to about 0·025 cm^3/g when the sample was saturated. In the case of the more heavily compressed sample IS(B), the maximum incremental pore volume of about 0·035 cm^3/g at the pore size of 10 μm reduced to approximately 0·020 cm^3/g when the sample was saturated. The saturation process also resulted in an increase in intra-aggregate pore sizes and this is clearly evident in the case of IS(B) as shown in Fig. 6(b). However, the full extent of this increase could not be established owing to limited range of pressure that could be applied to allow mercury to invade smaller voids in the aggregates.

Referring to Fig. 4, the samples exhibited swelling during the wetting process and the samples of IS(B) show approximately twice the magnitude of swell as the samples IS(A). The swelling of the samples is generated by the expansion of the aggregates. This expansion is clearly observable on sample IS(B) but less evident on sample IS(A). The inter-aggregate porosity would be expected to remain largely unchanged if expansion of the aggregates was the only mechanism for volume change. This simple scenario is illustrated graphically in Fig. 7(a). However, the experimental evidence presented in Fig. 6 indicates a significant reduction in the inter-aggregate pore volumes, and consequently porosity. This can only be explained by inferred distortion and expansion of the aggregates into the inter-aggregate pore spaces during wetting, leading to the observed reduction in the inter-aggregate pore size (Thom *et al.*, 2007). This scenario is presented graphically in Fig. 7(b). The ability of the aggregates to expand into the inter-aggregate pore spaces depends on how tightly the aggregates are initially packed. The more compact samples of IS(B) would have experienced considerably greater resistance to swelling into the inter-aggregates pore spaces compared with the aggregates of IS(A). Since both IS(A) and IS(B) were prepared at an identical initial specific water volume they would be expected to experience a similar amount of aggregate swelling during the wetting process. Since the aggregates of IS(B) faced stiffer resistance to swell into the inter-aggregate pore spaces, the consequence may be interpreted as the development of an enhanced thrusting force between the aggregates forcing the overall skeleton of the sample to expand. This resulted in greater overall volume change for samples IS(B), as shown in Fig. 4.

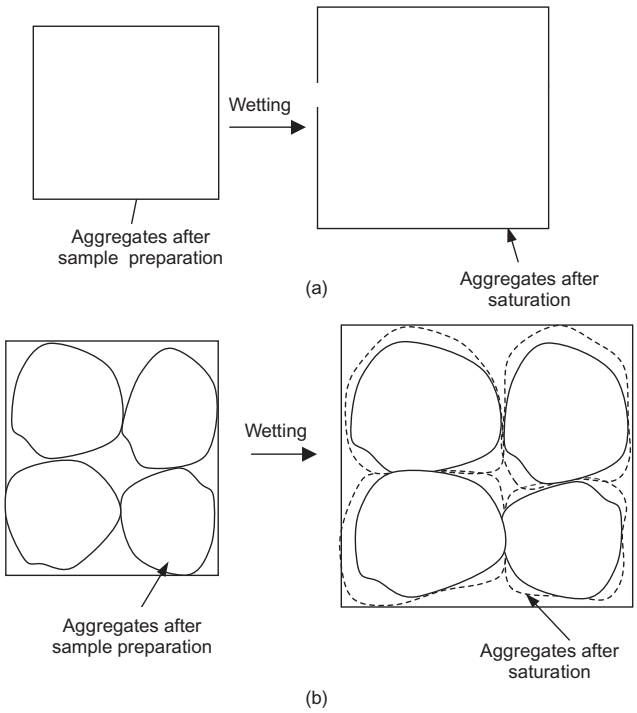

Fig. 7. Aggregate response during wetting of unsaturated soils: (a) simple model; (b) actual model – aggregates expanding into macro voids

Further important insight may be gained into the aggregated structure from the MIP results of Fig. 5. Since the pore size that separates the macro and micro voids is approximately 2 μm for both samples of IS(A) and IS(B), cumulative mercury intrusion measurements for the samples before wetting indicate that the volumes of mercury necessary to fill the inter-aggregate voids were approximately 0·180 cm^3/g and 0·125 cm^3/g respectively. These volumes correspond to a macro void ratio of approximately 0·493 and 0·331 for IS(A) and IS(B) respectively. The overall void ratios of these samples were 1·19 and 0·99 for IS(A) and IS(B) respectively. Therefore the magnitude of intra-aggregate void ratios of the samples IS(A) and IS(B) were 0·700 and 0·658 respectively. The kaolin aggregates were prepared at a water content of 25%. If the aggregates were saturated at the time of preparation and the inter-aggregates pores were free from water then the intra-aggregate void ratios of the samples would be approximately 0·663 taking the specific gravity of kaolin as 2·65. This value agrees favourably with the measured intra-aggregate void ratio from MIP results of IS(A) and IS(B), confirming the initial assumption of saturated aggregates.

The MIP results for saturated samples of IS(A) and IS(B) are also shown in Fig. 6. On a similar basis to the foregoing, the cumulative measurements of mercury intrusion indicate that the magnitudes of the inter-aggregate pore volumes were 0·150 cm^3/g and 0·080 cm^3/g for IS(A) and IS(B) respectively. These volumes correspond to inter-aggregate void ratios of 0·396 and 0·212. The overall average void ratios of the samples after saturation were 1·289 and 1·167 for IS(A) and IS(B) respectively. Therefore the intra-aggregate void ratios were respectively 0·89 and 0·95. The agreement between the two series of tests is reasonably good, indicating that aggregates of samples IS(A) and IS(B) expanded by approximately the same amount.

Effects of stress-induced anisotropy on the volume change of samples during wetting

Sivakumar & Wheeler (2000) and Wheeler & Sivakumar (1995) reported on a series of suction controlled tests on unsaturated soil samples prepared by statically compressing aggregated kaolin into a compaction mould to initial specific volumes of 2·19 and 1·99. The results from these tests on one-dimensionally compressed samples are referred to as ID(A) and ID(B) respectively and are compared with the data obtained from the present research. The conditions of the sample after equalisation are listed in Table 2.

The initial suctions in the samples of ID(A) and ID(B) were 830 kPa and 700 kPa respectively. Although paired samples identified as [IS(A),ID(A)] and [IS(B),ID(B)] were prepared at identical water contents and specific volumes, the initial suctions in the samples were significantly less in the case of the ID samples. The relationship between the specific water volume v_w and suction (suction plotted to a natural logarithm scale) for IS(A) against ID(A) and IS(B) against ID(B) during wetting are shown in Fig. 8. Though the paired samples were prepared at identical water contents there appear to be significant differences between the $v_w - s$ relationships shown in Fig. 8 with the ID(A) and ID(B) plots lying below the IS(A) and IS(B) plots respectively.

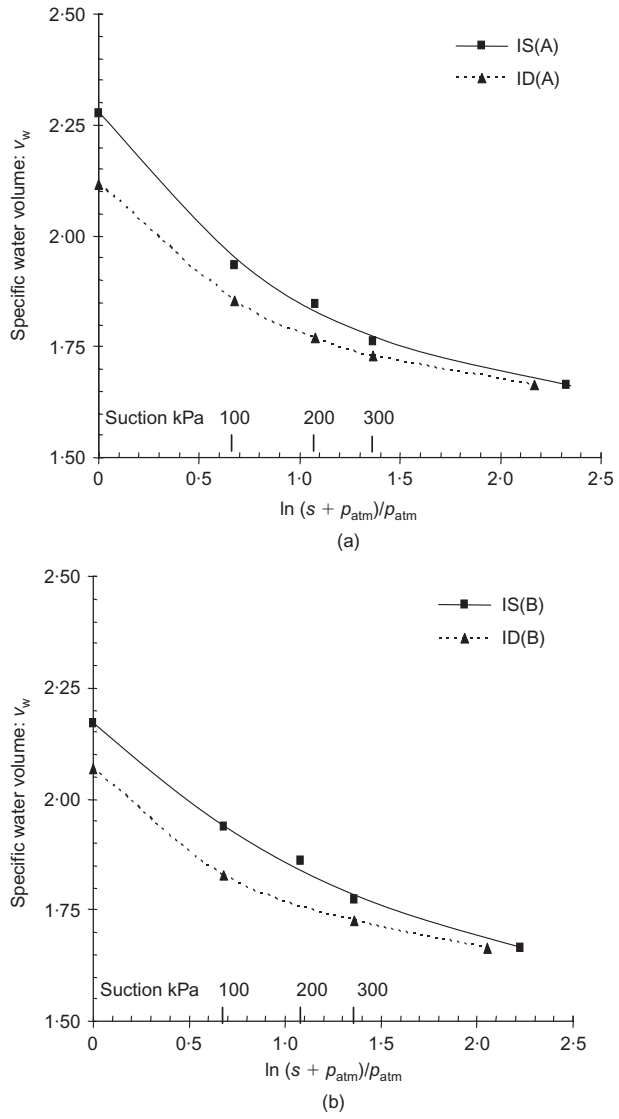

Fig. 8. Effects of stress-induced anisotropy on the specific water volume during wetting: (a) lightly compressed; (b) heavily compressed

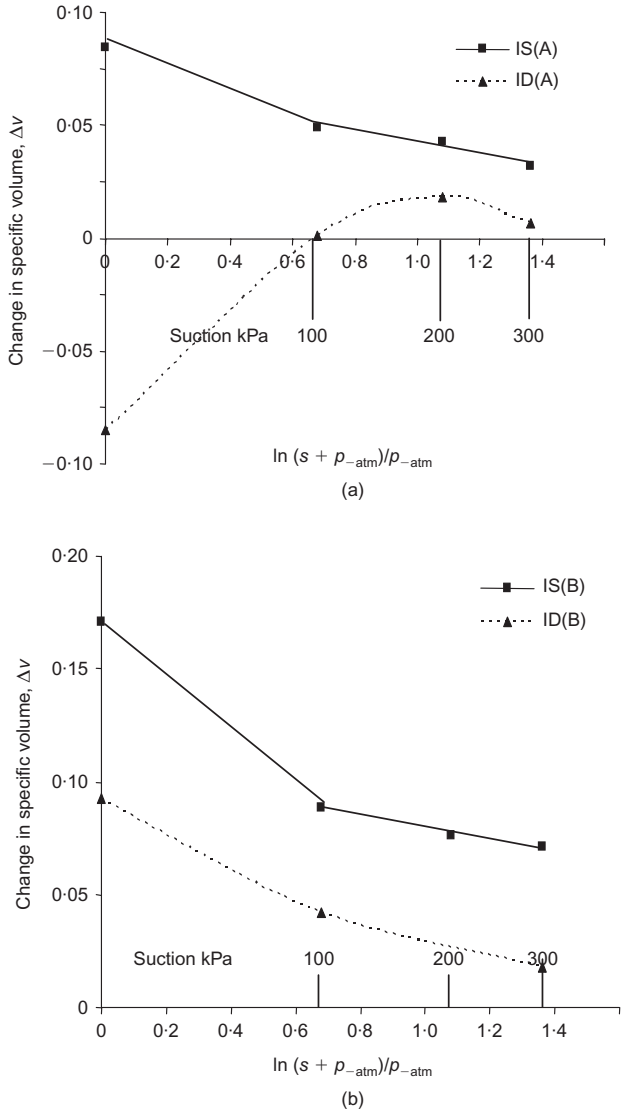

Fig. 9. Effects of stress-induced anisotropy on the specific volume during wetting: (a) low initial density; (b) high initial density

Figure 9 shows the change in specific volumes from initial conditions between the isotropically compressed and one-dimensionally compressed samples for both initial specific volumes of 2·19 (Fig. 9(a)) and 1·99 (Fig. 9(b)) during the reductions in suction. Although the paired samples had identical initial specific volumes and specific water volumes, the differences in the response of the samples to wetting are significant. In particular, the sample with isotropic previous stress history and relatively low initial density, IS(A), showed significant swelling during the wetting process whereas the sample with one-dimensional previous stress history, ID(A), exhibited significant collapse compression when the suction was reduced from 200 kPa to zero. The collapse compression is a result of a reduction in the larger inter-aggregate voids associated with decrease in the resistance to compression instigated by the wetting process. For the denser one-dimensionally prepared specimen ID(B) of Fig. 9(b), no collapse is indicated as the resistance to collapse is greater. Both IS(B) and ID(B) experienced swelling throughout the equalisation process though the plots differ significantly. The magnitude of swelling from the initial conditions was 85% greater in the case of the isotropically compressed sample than the one-dimensionally compressed sample.

The major questions that arise are

(*a*) why did the one-dimensionally compressed sample ID(A) exhibit collapse compression, whereas the sample with initially identical specific volume and specific water volume but with isotropic previous stress history, IS(A), exhibit only swelling?

(*b*) why did the isotropically prepared sample prepared using heavy compression, IS(B), exhibit significantly greater swelling than the paired one-dimensionally compressed sample with the same initial specific volume and specific water volume?

The observed behaviour will be discussed in the light of MIP results.

Effects of stress-induced anisotropy on the pore-size distribution of unsaturated samples following wetting

Figure 10 shows the MIP results of samples prepared using the two different methods. The results indicate the general trend of reduction in the larger inter-aggregate voids and increase in the smaller intra-aggregate voids following saturation from the as-prepared conditions. However, despite the identical initial specific volumes and specific water

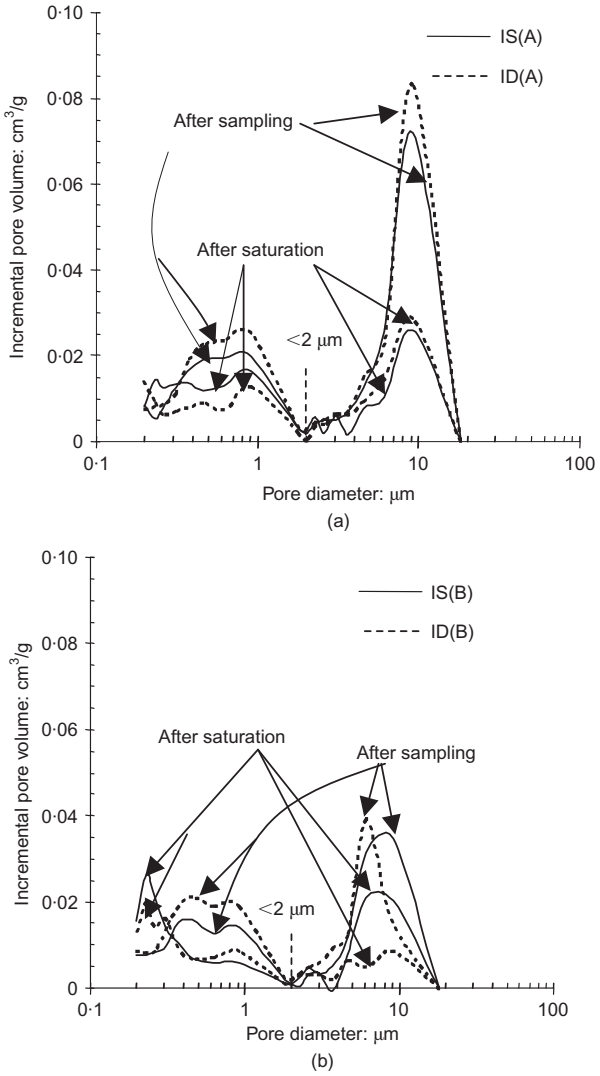

Fig. 10. Effects of stress-induced anisotropy on the pore size distribution: (a) lightly compressed; (b) heavily compressed

volumes, the samples with isotropic and one-dimensional previous stress history exhibited slightly different initial bimodal pore size distributions, represented in the figure as 'after sampling'. The samples prepared using one-dimensional compression (ID) are shown to exhibit a slightly more 'open' macro-structure at both levels of initial compression effort (i.e., light ID(A) and heavy ID(B) compression). The open structure exhibited by the statically compressed sample of ID(A) may have contributed to unstable inter-aggregate contacts susceptible to collapse during wetting. However, the observed small difference in the pore size distributions does not explain satisfactorily the disparity in the volume change behaviour reported in Fig. 9 other than to suggest that small differences in structure may result in significantly different behaviour characteristics consistent with unstable or metastable conditions.

Figure 10 also shows the pore size distributions of samples of IS(A), ID(A), IS(B) and ID(B) following the saturation process. Sample IS(A) shows a significant reduction in the inter-aggregate voids compared with the more compact sample IS(B). As demonstrated earlier, for the less densely compacted specimens, IS(A), uptake of water resulted in expansion of the aggregates into the inter-aggregate voids, thus their closure, whereas for the more compact samples, IS(B), there was a greater overall sample expansion on uptake of water as there was less inter-aggregate void space to allow for expansion of the aggregates. This observation differs from the response of the one-dimensionally compressed samples (i.e. ID(A) and ID(B)) where the reductions in the inter-aggregate pore spaces are more significant in both cases. In the case of sample ID(B), the saturation process appears to have nearly eradicated the presence of a bimodal distribution. This ties in with the observation in Fig. 9 that the isotropically prepared, heavily compressed samples IS(B) exhibited significantly greater swelling than one-dimensionally compressed samples ID(B), as the larger inter-aggregate voids in the latter samples closed up during the saturation process reducing the overall sample swelling. This appears to suggest a degree of breakdown of the aggregations. The behaviour is notably different to that suggested by the pore size distributions for samples IS(A) and IS(B), and indeed by the more lightly compacted sample ID(A), where, after saturation, a bimodal distribution is still evident (Fig. 10(a)). If the aggregates are visualised as 'spherical' prior to the sampling process, one-dimensional static compression will have resulted in the aggregates undergoing shear deformation leading to a more lenticular aggregate appearance. The process may have inflicted a degree of fissuring or fracturing of the aggregates, making them susceptible to degradation upon saturation, since the initial water content at the time of preparation was at least 9% less than the plastic limit (PL = 34%) of kaolin.

Pressure–volume relationship during isotropic compression under controlled and variable suctions of samples prepared isotropically

Following swelling of isotropically prepared samples to predefined suction values, samples were isotropically compressed under a mean net stress by ramping in stages. Fig. 11 shows the specific volume plotted against mean net stress for samples of IS(A) and IS(B) isotropically compressed at zero, 100, 200 and 300 kPa suction respectively. The state parameters after isotropic compression are listed in Table 1. The observations made are outlined below.

Yielding. There is a clear yield stress which can be identified by a marked change in the slope of the continuous plot of the specific volume against the logarithm of mean net stress. As expected, the estimated yield stress of samples increases with increasing suction. For IS(A) these are 62 kPa, 105 kPa, 155 kPa and 210 kPa at zero, 100, 200 and 300 kPa of suction respectively. The estimated values of yield stress for samples of IS(B) are 80 kPa, 210 kPa, 315 kPa and 440 kPa at zero, 100, 200 and 300 kPa of suction respectively. The yield stresses are plotted against suction to form the LC yield locus shown as solid data points in Fig. 12. Since the samples of IS(B) were subjected to higher compression pressures during initial formation, they resulted in greater yield stresses than those for samples IS(B).

While the yield stress increasing with increasing suction agrees with other published results (Alonso *et al.*, 1990; Maãtouk *et al.*, 1995; Wheeler & Sivakumar, 1995; Cui & Delage, 1996; Futai & Almeida, 2005), the shape of the yield locus is interesting. The yield locus shown in Fig. 12 is not a curve but a straight line. This contradicts proposals and experimental evidence by other researchers, including Sivakumar & Wheeler (2000) and Wheeler & Sivakumar (1995), and which were based on the findings from one-dimensionally compressed samples. The increase in the initial compression pressure from 400 kPa, used in preparing samples of IS(A), to 800 kPa, used in the case of preparing samples of IS(B), has approximately doubled the yield stress at each value of suction except at zero suction.

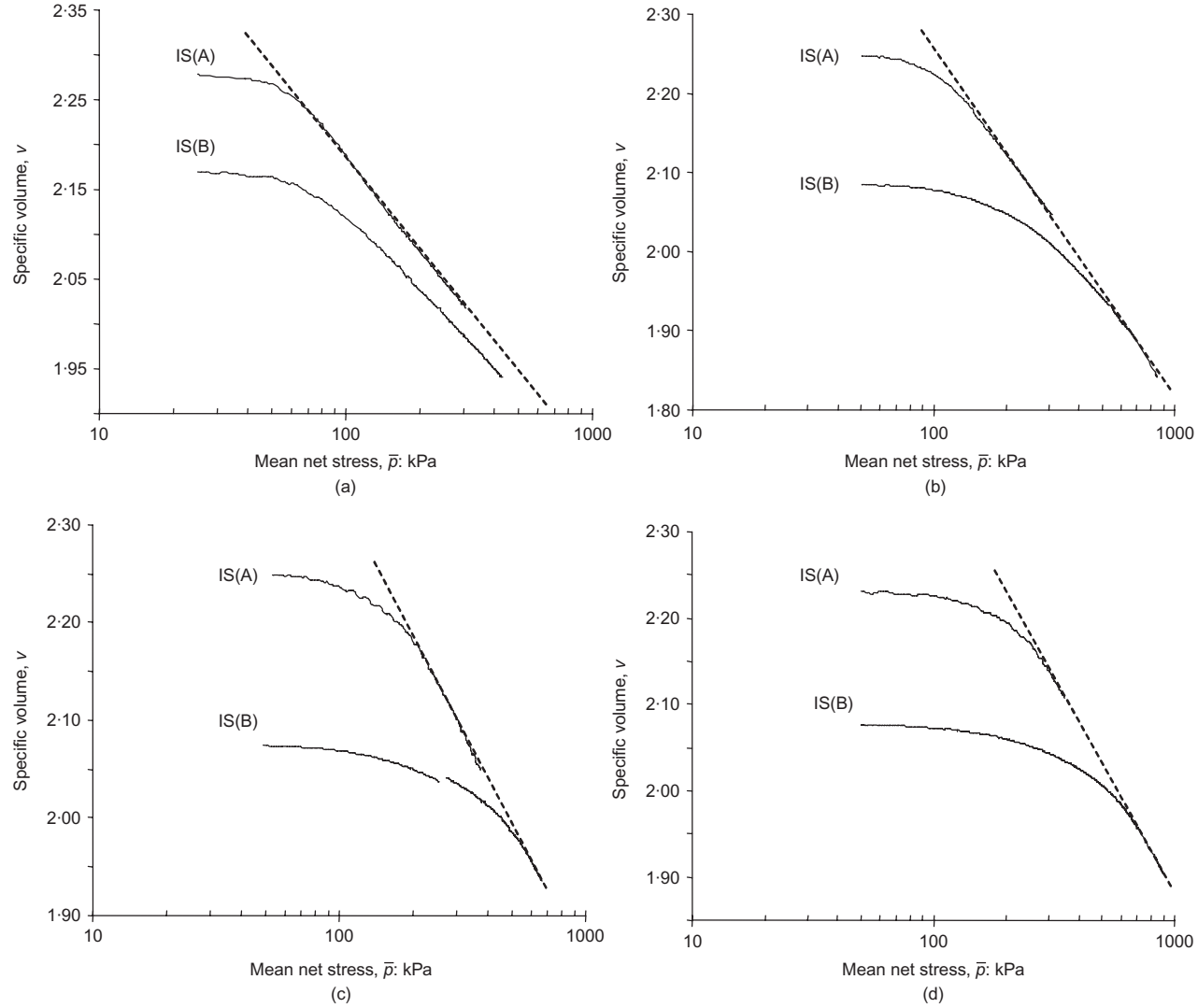

Fig. 11. Pressure–volume relationships of samples with isotropic previous stress history: (a) $s = 0$; (b) $s = 100$ kPa; (c) $s = 200$ kPa; (d) $s = 300$ kPa

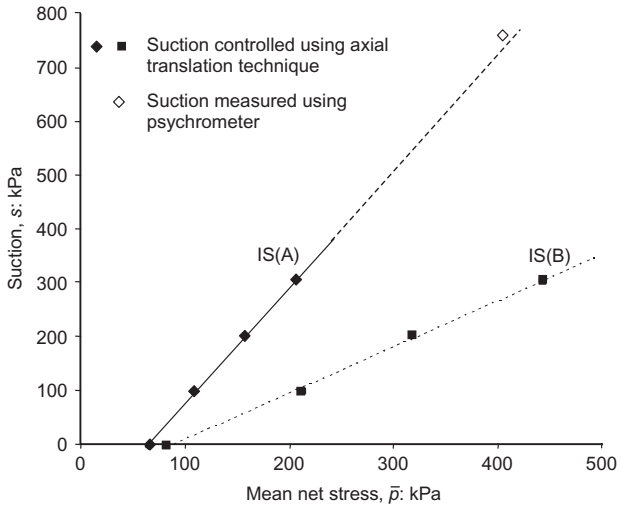

Fig. 12. Loading–collapse yield locus

Figure 13(a) shows the $v - \overline{p}$ relationship obtained from compression tests carried out under constant water mass conditions. The suction in this case was measured using a psychrometer and its variation is also shown in Fig. 13(b). At the point of yielding the suction and mean net stress were 780 and 400 kPa respectively and this point is also included in the LC yield locus in Fig. 12 using an open data point. The linearity of the LC yield locus is further substantiated by this evidence.

Unique normal compression surface. Continuous plots of specific volume versus mean net stress are presented in Fig. 11. This information was used to determine the values of the slope $\lambda(s)$ and intercept $N(s)$ of the normal compression lines (with $N(s)$ specified at $\overline{p} = p_{atm} = 100$ kPa).

Many researchers have postulated the existence of consistent compression characteristics for unsaturated soils (Alonso *et al.*, 1990; Maãtouk *et al.*, 1995; Wheeler & Sivakumar, 1995; Cui & Delage, 1996; Sivakumar & Wheeler, 2000; Futai & Almeida, 2005). In order to validate this postulation it is necessary to confirm that the state of an unsaturated soil on yielding remains on a unique normal compression line for a given value of suction, and on a unique compression surface when the effect of suction is considered. Sivakumar & Wheeler (2000) reported that an increase in initial compaction effort produced different normal compression lines (or surfaces when extended to take account of suction). This view has also been expressed by other researchers

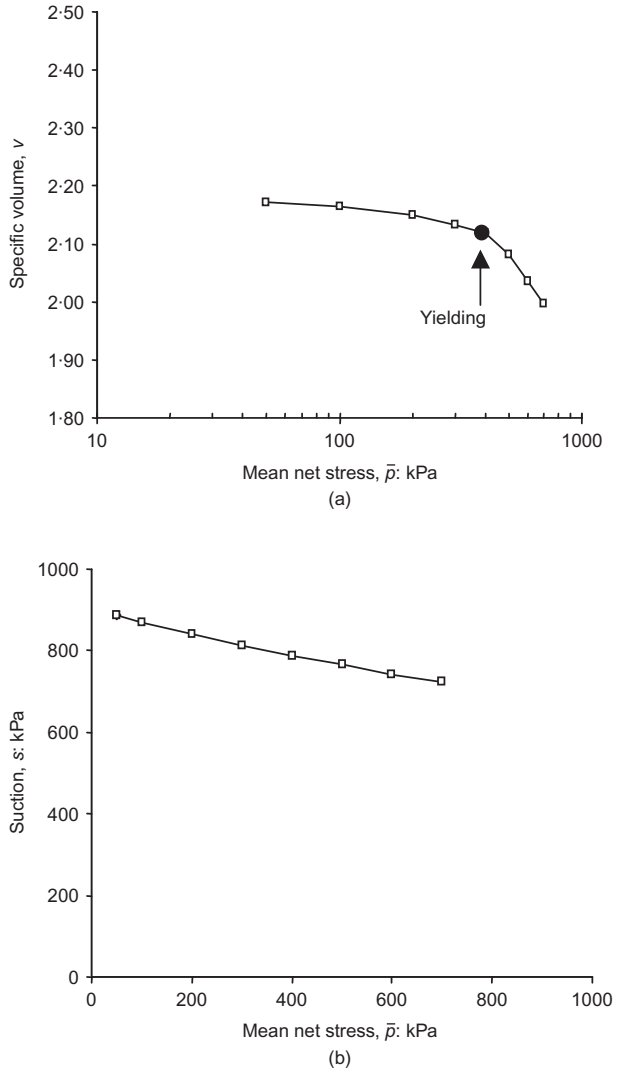

Fig. 13. Isotropic compression under constant water mass conditions (IS(A))

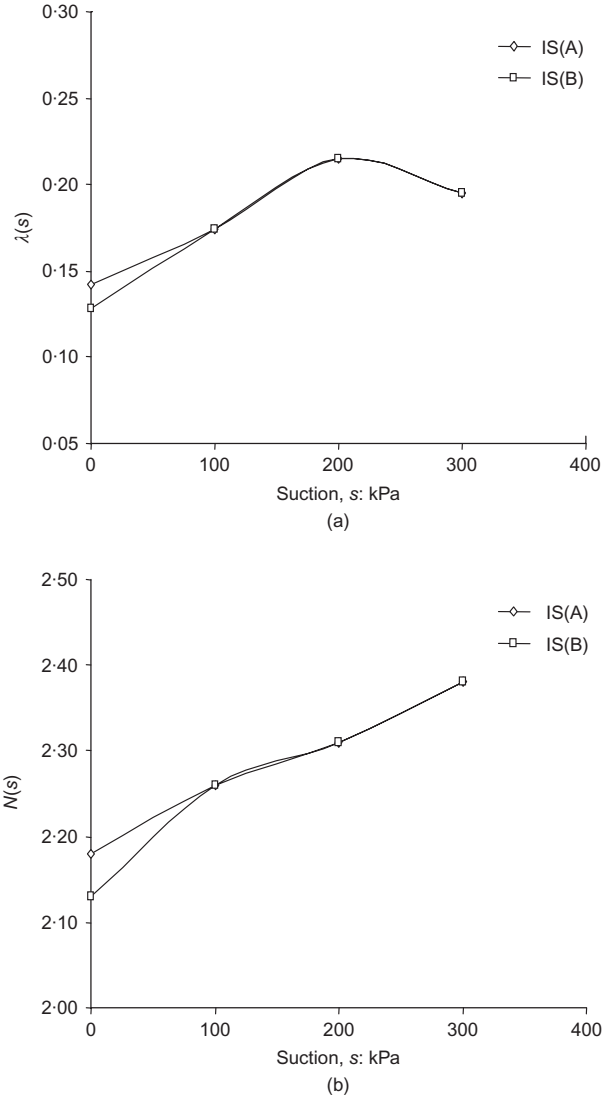

Fig. 14. Variation of $N(s)$ and $\lambda(s)$ with suction

(Estabragh *et al.*, 2004; Maãtouk *et al.*, 1995). Sivakumar & Wheeler (2000) explained the differences in the position of the normal compression surface using the concept of rotational hardening. The experimental evidence obtained as part of the research reported here provides strong experimental evidence to suggest that, for isotropically compressed samples, the line at each value of suction is unique regardless of the initial condition of the sample. Fig. 11 shows that the pressure–volume curves of IS(A) merge with corresponding curves of IS(B) (except for a small shift at zero suction) when the samples have fully yielded to overcome the previous stress history generated by the preparation process.

Figure 14 shows the variations of slope, $\lambda(s)$, and intercept, $N(s)$, of the normal compression line for both series of samples. Both $\lambda(s)$ and $N(s)$ are dependent on suction and independent of initial specific volume. The slope $\lambda(s)$ is shown to increase with increasing suction up to $s = 200$ kPa and reduce with further increase in suction. While this finding is in reasonable agreement with Wheeler & Sivakumar (1995), it contradicts the original proposal made by Alonso *et al.* (1990) and the experimental findings of Cui & Delage (1996) on unsaturated compacted silt, who suggested a continuous reduction in the slope of the normal compression line.

Effects of stress-induced anisotropy on the pressure–volume relationship and yielding

The pressure–volume responses of the samples IS(A) and ID(A) are shown in Figs 15(a) and 15(b) for suction values of 100 kPa and 300 kPa respectively and those for IS(B) and ID(B) are shown in Figs 15(c) and 15(d) for similar suctions respectively. The approximate positions of the normal compression lines are shown by broken lines. In the case of IS(A) and ID(A) there appears to be no significant difference in the slope of the normal compression lines, when the suction value was 100 kPa. However differences do exist for a suction of 300 kPa. In the case of IS(B) and ID(B) the differences in the slope of the compression lines are significant at both values of suction. The slopes of the normal compression line in the case of ID(B) samples are considerably smaller than of IS(B). The reason for this difference lies in the development of rotational hardening in one-dimensionally compressed samples. A detailed discussion on this is given in Sivakumar & Wheeler (2000).

The yield stresses of one-dimensionally compressed samples and isotropically prepared samples are shown in Fig. 16. Although both isotropically and one-dimensionally compressed samples had identical initial specific volumes and specific water volumes, the suction equalisation process generated significant changes in the pore size distributions and thus changes in the specific volumes at the beginning of

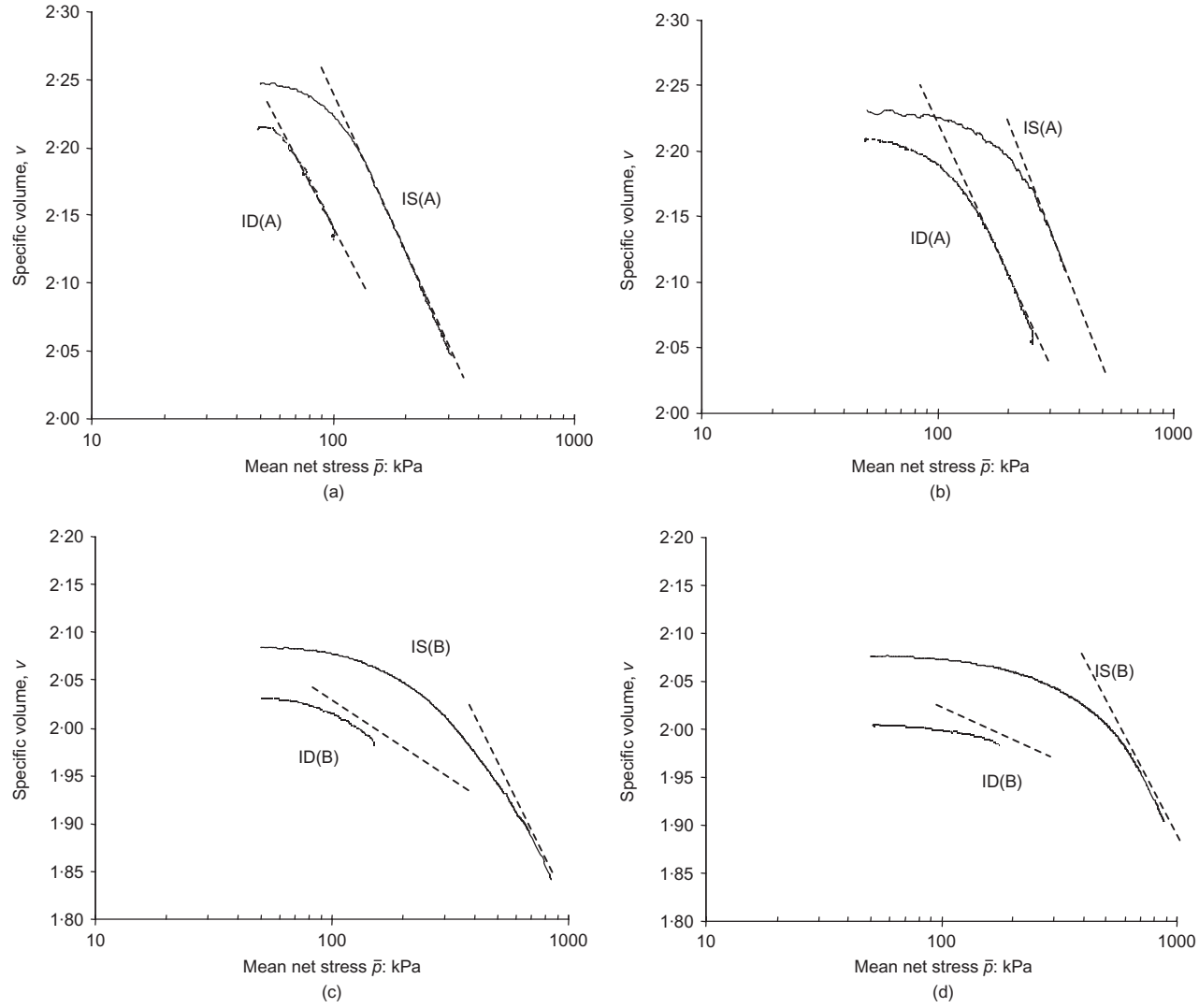

Fig. 15. Effects of stress-induced anisotropy on the pressure–volume relationship during isotropic compression: (a) $s = 100$ kPa; (b) $s = 300$ kPa; (c) $s = 100$ kPa; (d) $s = 300$ kPa

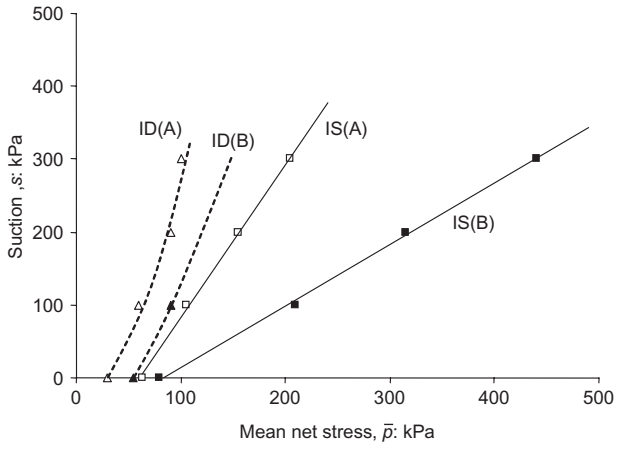

Fig. 16. Effects of stress-induced anisotropy on the LC yield locus

isotropic compression. The consequence is that the LC yield loci for isotropic compression of ID(A) and ID(B) lie below those of IS(A) and IS(B) (Fig. 16). The yield stresses of isotropically compressed samples at each value of suction are thus significantly higher than those of the paired one-dimensionally compressed samples. The yield stress at a given suction increases with compression pressure used during sampling regardless of the nature of the sample preparation (i.e., ID or IS). However, the magnitude of the increase is strongly determined by the initial soil structure. ID(A) and ID(B) yielded at stresses of 60 and 90 kPa respectively at a suction value of 100 kPa. In contrast, at the same suction value, IS(A) and IS(B) yielded at stresses of 105 and 210 kPa respectively. Samples IS(A) and IS(B) with isotropic stress history produced LC yield loci that are reasonably straight lines in the s: $\overline{p}$ plane. However, the samples of ID(A) prepared to a one-dimensional stress history are shown to produce LC yield loci which are non-linear, with the curves having similar shapes to those proposed by Alonso *et al.* (1990). Similar conclusions can be drawn for the case of ID(B) though there are only two data points available to justify the statement.

The positions of yield loci for both one-dimensionally compressed and isotropically compressed samples are outlined schematically in the q: $\overline{p}$ plane in Fig. 17. It is reasonable to assume that the shape of the yield locus for initially isotropically compressed specimens is an ellipse and parallel to the mean net stress axis (this is discussed in the companion paper (Sivakumar *et al.*, 2010)). It is also reasonable to assume that a one-dimensionally compacted specimen will have inherited a certain degree of stress-induced anisotropy

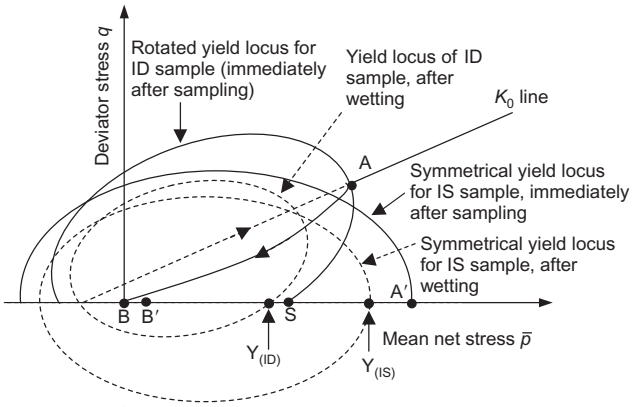

Fig. 17. The effects of anisotropy on the yield locus in q: $\bar{p}$ plane

from the previous loading history thus the yield locus is rotated away from the mean net stress axis. It is possible to present a plausible explanation of the observations in terms of yield surfaces in $q - \bar{p}$. The one-dimensionally compressed samples will have inherited a rotated yield locus, which is shown as passing through point A on the K_0 line (note that the position of the K_0 line in unsaturated soil is yet to be understood, but for convenience it is assumed to be parallel to the K_0 line for saturated soils though not passing through the origin). This yield locus intersects the $\bar{p}$ axis at S. Path AB represents unloading where the one-dimensional loading during sampling was removed (mean net stress $\bar{p}$ is zero at this stage). Path BB′ represents reloading of the sample under isotropic stress conditions in the testing chamber and allowed to go through the wetting process where the suction was reduced. The reduction in the suction on wetting is conjectured as various values under mean net stress of 50 kPa, instigating a reduction in the size of the yield locus and the new yield locus at a pre-selected suction passes through point $Y_{(ID)}$ on the $\bar{p}$ axis. It is assumed that the soil still exhibits some degree of anisotropy and therefore the yield locus is still rotated. The isotropically compressed samples should have inherited a yield locus that passes through A′ and is symmetrical about the $\bar{p}$ axis (Wheeler & Sivakumar, 2000). The reduction in suction is conjectured as leading to shrinkage in the size of the yield locus and the new yield locus at the pre-selected suction value passes through point $Y_{(IS)}$. It is assumed that this sample still exhibits a symmetrical yield locus. Therefore the isotropic compression of the samples in the testing chamber, which have had one-dimensional and isotropic previous stress histories will yield at points $Y_{(ID)}$ and $Y_{(IS)}$ respectively. Based on the foregoing scenario, qualitatively the sample with one-dimensional previous stress history would be expected to yield at a smaller mean net stress than that of a sample with isotropic previous stress history. This is demonstrated by experimental evidence.

CONCLUSIONS

The paper describes a detailed testing programme and analysis carried out on samples of unsaturated kaolin with isotropic and anisotropic properties. The testing allows the basic propositions in constitutive modelling to be assessed together with evaluation of the effects of anisotropy on the overall behaviour of the soil. The samples were wetted to various values of suction and subsequently isotropically compressed. MIP study was also undertaken to assess the effects of wetting on the pore size distribution.

MIP study has revealed that the samples with a one-dimensional loading history at the time of sampling inherited an unstable structure which is not shown by samples with isotropic loading history. This is one of the possible reasons for the substantial collapse compression observed during the wetting of some samples. The samples with isotropic stress history at the time of sampling exhibited substantial swelling and the magnitude of swelling was influenced by the inter-aggregate void ratio. The more heavily compacted a specimen, the greater the swelling, with implications on the behaviour of compacted unsaturated fills.

The results obtained from the samples which inherited isotropic previous stress history have shown, probably for the first time, the existence of a unique normal compression surface that is not dependent on the initial conditions of the samples. However the existence of this surface was less obvious in the case of samples with a one-dimensional loading history. Significant differences were also observed in terms of yielding of samples with two different stress histories. The shape and the size of the LC yield locus were remarkably different.

ACKNOWLEDGEMENTS

The authors would like to thank Dr Gabriel Gallagher (Glover Site Investigation Limited, Northern Ireland), K. V. Senthilkumaran and P. J. Carey (P. J. Careys Contractors, UK) and J. Vimalan (VJ Tech Ltd, Reading, UK) for unconditional financial contributions to support geotechnical research at Queen's University Belfast.

NOTATION

e	void ratio
G_s	specific gravity
K_0	coefficient of earth pressure at rest
$N(s)$	intercept of normal compression line in v-ln $\bar{p}$ plot
$\bar{p}$	mean net stress
$p_{\text{-atm}}$	atmospheric pressure
q	deviator stress
s	matric suction
s_{ref}	reference suction
u_a	pore air pressure
u_w	pore water pressure
w	water content
v	specific volume
v_w	specific water volume
κ_s	elastic swelling index with respect to $\bar{p}$
$\lambda(s)$	slope of normal compression line in v-ln $\bar{p}$ plot
σ_1	major principal stress
σ_3	minor principal stress

REFERENCES

Ahmed, S., Lovell, C. W. & Diamond, S. (1974). Pore sizes and strength of compacted clay. *J. Geotech. Engng Div.* **GT4**, 407–425.

Alonso, E. E., Gens, A. & Hight, D. W. (1987). Special problem soils: General Report. *Proc. 9th Eur. Conf. Soil Mech., Dublin*, 1087–1146.

Alonso, E. E., Gens, A. & Josa, A. (1990). A constitutive model for partially saturated soils. *Géotechnique* **40**, No. 3, 405–430.

Alonso, E. E., Lloret, A. & Gens, A. (1995). Experimental behaviour of highly expansive double-structure clay. *Proc. 1st Int. Conf. Unsaturated Soils, Paris*, **1**, 11–16.

American Society for Testing and Materials (2004). *Standard test method for determination of pore volume and pore volume distribution of soil and rock by mercury intrusion porosimetry*, D4404-84. West Conshohocken, PA, USA: ASTM. Available from www.astm.org.

Comstock, J. P. (2000). Correction of thermocouple psychrometer readings for the interaction of temperature and actual water potential. *Crop Sci*. **40**, No. 3, 709–712.

Cui, Y. J. & Delage, P. (1996). Yielding and plastic behaviour of

an unsaturated compacted silt. *Géotechnique* **46**, No. 2, 291–311.

Delage, P. & Graham, J. (1995). Mechanical behaviour of unsaturated soils: Understanding the behaviour of unsaturated soils requires reliable conceptual models. *Proc. 1st Int. Conf. Unsaturated Soils, Paris*, **3**, 1223–1256.

Delage, P., Audiguier, M., Cui, Y. J. & Howat, M. D. (1996). Microstructure of a compacted silt. *Can. Geotech. J.* **33**, 150–158.

Estabragh, A. R., Javadi, A. A. & Boot, J. C. (2004). Effect of compaction pressure on consolidation behaviour of unsaturated silty soil. *Can. Geotech. J.* **41**, 540–550.

Futai, M. M. & Almeida, M. S. S. (2005). An experimental investigation of the mechanical behaviour of an unsaturated gneiss residual soil. *Géotechnique* **55**, No. 3, 201–213.

Gens, A. & Alonso, E. E. (1992). A framework for the behaviour of unsaturated expansive clays. *Can. Geotech. J.* **29**, 1013–1032.

Graham, J. & Houlsby, G. T. (1983). Anisotropic elasticity of a natural clay. *Géotechnique* **33**, No. 2, 165–180.

Hilf, J. W. (1956). *An investigation of porewater pressure in compacted cohesive soils*. Technical memorandum 654. Denver: US Bureau of Reclamation.

Leroueil, S. & Vaughan, P. R. (1990). The general and congruent effects of structure in natural soils and weak rocks. *Géotechnique* **40**, No. 3, 467–488.

Maãtouk, A., Leroueil, S. & La Rochelle, P. (1995). Yielding and critical state of a collapsible unsaturated silty soil. *Géotechnique* **45**, No. 3, 465–477.

Matayas, E. L. & Rahadakishna, H. S. (1968). Volume change characteristics of partially saturated soils. *Géotechnique* **18**, No. 4, 432–448.

Muir Wood, D. (1990). *Soil behaviour and critical state soil mechanics*. 1st edn. Cambridge: Cambridge University Press.

Schofield, A. N. & Wroth, C. P. (1968). *Critical state soil mechanics*. London: McGraw-Hill Book Company.

Sharma, R. S. (1998). *Mechanical behaviour of unsaturated highly expansive clays*. PhD thesis, University of Oxford.

Sivakumar, V. (1993). *A critical state framework for unsaturated soil*. PhD thesis, University of Sheffield.

Sivakumar, V., Doran, I. G. & Graham, J. (2002). Particle orientation and its influence on the mechanical behaviour of isotropically consolidated reconstituted clay. *Engng Geol.* **66**, No. 3–4, 197–209.

Sivakumar, V. & Wheeler, S. J. (2000). Influence of compaction procedure on the mechanical behaviour of an unsaturated compacted clay, Part 1: Wetting and isotropic compression. *Géotechnique* **50**, No. 4, 359–368.

Sivakumar, R., Sivakumar, V., Blatz, J. & Vimalan, J. (2006). Twin-cell stress path apparatus for testing unsaturated soils. *Geotech. Testing J.*, **29**, No. 2, 1–5.

Sivakumar, V., Sivakumar, R., Boyd, J. & Mackinnon, P. (2010). Mechanical behaviour of unsaturated kaolin (with isotropic and anisotropic stress history). Part 2: performance under shear loading. *Géotechnique* doi: 10.1680/geot.8.P.008.

Tan, W. C. (2004). *Wetting, drying, compression and shear strength characteristics of compacted clay.* PhD thesis, Queen's University Belfast, UK.

Thom, R., Sivakumar, R., Murray, E. J. & Mackinnon, P. (2007). Pore size distribution of unsaturated compacted kaolin: the initial states and final states following saturation. *Geotechnique* **57**, No. 5, 469–474.

Thom, R., Sivakumar, V., Brown, J. & Hughes, D. (2008). A simple triaxial system for evaluating the performance of unsaturated soils under repeated loading. *Geotech. Testing J.* **31**, No. 2, 1–8.

Wan, A. W. L., Gray, M. N. & Graham, J. (1995). On the relations of suction, moisture content and soil structure in compacted clays. *Proc. 1st Int. Conf. Unsaturated Soils, Paris*, **1**, 215–222.

Wang, Q., Pufahl, D. E. & Fredlund, D. G. (2002). A study of critical state on an unsaturated silty soil. *Can. Geotech. J.* **39**, No. 1, 213–218.

Washburn, E. W. (1921). Note on a method of determining the distribution of pore sizes in a porous material. *Proc. Nat. Acad. Sci. U.S.* **7**, No. 4, 115–116.

Wheeler, S. J. (1997). A rotational hardening elasto-plastic model for clays. *Proc.4th Int. Conf. Soil Mech. Found. Engng, Hamburg*, **1**, 431–434.

Wheeler, S. J. & Sivakumar, V. (1995). An elasto-plastic critical state framework for unsaturated soil. *Géotechnique* **45**, No. 1, 35–53.

Wheeler, S. J. & Sivakumar, V. (2000). Influence of compaction procedure on the mechanical behaviour of an unsaturated compact clay. Part 2: shearing and constitutive modelling. *Géotechnique* **50**, No. 4, 369–376.